

Electronic supplementary information (ESI) for

Inelastic neutron scattering study of a glass-forming liquid in soft confinement

Reiner Zorn, Maria Mayorova, Dieter Richter, and Bernhard Frick

1 Elastic neutron scattering

1.1 Small-angle neutron scattering (SANS)

SANS experiments were carried out on the SANS machine KWS-1 at Forschungszentrum Jülich. The instrument was used with an incident wavelength of 7 Å and detector distances of 1.25 m and 2 m yielding a Q range of 0.023...0.25 Å⁻¹. In order to see the PG core dimension preferentially, the hdd microemulsion was used for this purpose. Because the scattering length density of PG ($0.13 \times 10^{10} \text{ cm}^{-1}$) is much more different from that of d-decalin ($6.00 \times 10^{10} \text{ cm}^{-1}$) than is that of d-AOT ($7.19 \times 10^{10} \text{ cm}^{-1}$) the scattering from the shell is weighted roughly by 0.04 with respect to the core. This simplifies the evaluation because the simple form factor of a sphere can be used. As a background the scattering of pure d-decalin was subtracted.

1.2 Neutron diffraction with polarisation analysis

To extend the Q range the neutron spectrometer with polarisation analysis DNS at Forschungszentrum Jülich was used. Using an incident wavelength of 5.73 Å this instrument has a Q range of 0.16...2.34 Å⁻¹. The additional advantage of this instrument is that thanks to the polarisation analysis coherent and incoherent scattering can be separated. In the SANS experiment this can only be done approximately using a background sample (see above).

2 Inelastic neutron scattering

2.1 Time-of-flight neutron scattering spectroscopy

Time-of-flight (TOF) neutron scattering experiments have been done on three different instruments listed in Table 1. The specifications of all TOF instruments are similar. The resolution depends on the scattering angle because of flight-path differences. (Hollow cylindrical samples were used.) The main difference for NEAT is that in contrast to the other TOF spectrometers it does the wavelength selection by choppers. Therefore, the resolution function has less pronounced wings at the same nominal width. FOCUS is installed at a spallation source, SINQ. But because SINQ is a continuous source and the

instrument constructed in direct geometry, from the user perspective there is no difference to a reactor instrument. The resolutions of all TOF spectrometers correspond to a limit of 20...30 ps in the time domain after Fourier transform (see below). The maximal energy transfer used in the Fourier transform was 2...10 meV. There, the kinematic restriction limits the E range for low Q while for high Q the limit results from the decreasing accuracy of the data. This maximum E imposes a short time limit of 0.2...0.9 ps after Fourier transform depending on Q .

2.2 Backscattering neutron spectroscopy

Two backscattering spectrometers (BS) were used which both have a very similar construction: The neutrons are selected and analysed by (unpolished) Si wafers in 111 orientation. Therefore the wavelength is always 6.271 Å the full width at half maximum of the resolution function about 1 μ eV, and the Q range up to 1.9 Å⁻¹. In most cases the data presented originate from IN16 at Institut Laue-Langevin in Grenoble, France. The elastic scans and some of the inelastic spectra for the microemulsion were obtained on the spectrometer PI at Forschungszentrum Jülich, Germany. The main difference between the two instruments is that IN16 has a higher intensity and its resolution function is closer to a Gaussian while that of PI has noticeable algebraic wings. In addition, the background on IN16 is lower by an order of magnitude. Fourier transform of the spectra leads to reliable data only in the time range from 150 ps to 2...3 ns.

3 Approximate estimation of vibrational density of states

Because the inelastic incoherent neutron scattering in *classical* one-phonon approximation is proportional to the vibrational density of states (VDOS) divided by the squared frequency, $g(\omega)/\omega^2$, it is possible to extract the approximate VDOS from neutron scattering spectra without additional assumptions. Just to get a rough idea of the vibrational spectrum it is allowed to average all available detectors of an instrument because the Q dependence is trivial if multiple scattering is neglected ($\propto Q^2$). This has been done in Fig. 1 for all detectors with angles $> 34^\circ$. The lowest-angle detectors have been omitted because they contain small-angle scattering from the microemulsion structure.

Already from this crude evaluation it can be seen that in the case of bulk PG there is a well developed maximum around 3 meV. This deviation from the Debye VDOS, which should give a constant in this representation, is typical for amorphous materials. It is usually called ‘boson peak’ (BP). In comparison, the confined spectrum does not show a peak but also not a constant value in the observed energy transfer range. From the spectrum of the hdd microemulsion before subtraction of the ddd data it can be seen that this correction is rather large. Nevertheless, a possible variation of $\pm 10\%$ in the factor

Table 1: Main specifications of the inelastic neutron scattering spectrometers used in this study. The institutions are ILL: Institut Laue-Langevin, Grenoble, France; BENS: Berlin Neutron Scattering Center, Hahn-Meitner-Institut, Berlin, Germany; and SINQ: Swiss Spallation Neutron Source, Paul-Scherrer Institut, Villigen, Switzerland; FZJ: Forschungszentrum Jülich, Germany. FWHM: full width of the elastic line at half maximum.

Type:	IN6	NEAT	FOCUS	IN16	PI
Institution:	TOF	TOF	TOF	BS	BS
Incident wavelength [Å]:	ILL	BENS	SINQ	ILL	FZJ
Resolution FWHM [μeV]:	5.12	5.5	4.85	6.271	6.271
max. energy transfer useable for FT [meV]:	85...110	101...129	106...175	0.93	1.03
max. Q [Å^{-1}]:	2...10	2...10	2...10	0.014	0.017
	2.1	2.1	2.3	1.9	1.9

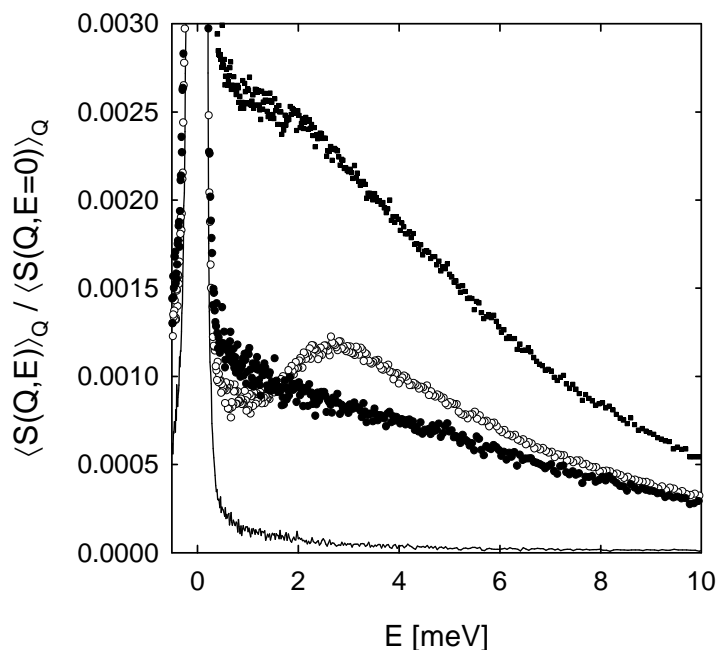


Figure 1: Spectra from time-of-flight spectrometer Focus. Filled circles: PG in soft confinement (100 K), empty symbols: bulk PG (100 K), lines: resolution (bulk, 5 K), filled squares: hdd microemulsion without subtraction of ddd (100 K). Spectra of all detectors in the scattering angle range $34 \dots 126^\circ$ were summed up. Each spectrum is normalised to its elastic maximum with exception of the hdd spectrum which is normalised to the maximum after subtraction of ddd to show it on the same scale as the spectrum of confined PG.

for the subtraction would not qualitatively change the result of absence of the BP in the spectra of confined PG.

4 Elastic scans

To obtain a quick overview of the temperature dependence of the microscopic dynamics an *elastic scan* can be performed on a neutron backscattering spectrometer. In this mode of operation the energy transfer is fixed to zero and the (elastic) scattering is recorded while changing the temperature. In Gaussian approximation the elastic *incoherent* intensity should depend on the mean-square displacement of the scatterers (here mainly hydrogen atoms) only:

$$I(Q, T) = I_0(Q) \exp\left(-\frac{\langle r^2 \rangle(T)}{6} Q^2\right). \quad (1)$$

Here I_0 is the elastic incoherent intensity without any dynamics. It is usually replaced by that at a certain low temperature (e.g. 4 K) with the consequence that the mean-square

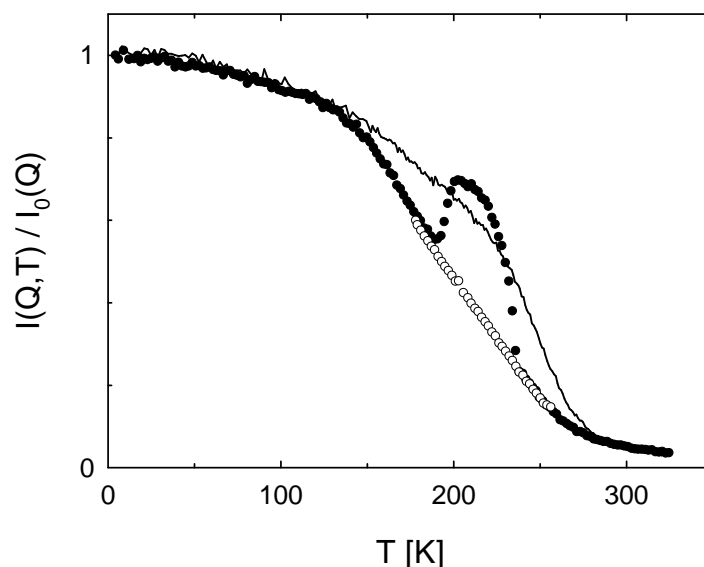


Figure 2: Elastic scans. The scattering vector corresponds to the average of the two highest-angle detectors, roughly $Q = 1.8 \text{ \AA}^{-1}$. Continuous line: bulk PG; filled symbols: hdd microemulsion heating scan; hollow symbols: hdd microemulsion cooling scan.

displacement is that excluding quantum zero-point motions. It also has to be noted that for diffusion-like processes $\langle r^2 \rangle$ increases continuously with time. In that case the effective $\langle r^2 \rangle$ calculated from the data is determined by the resolution of the instrument. In case of the backscattering spectrometers used here the time scale is roughly [1] $2\hbar/\Delta E$, where $\Delta E = 1 \mu\text{eV}$ is the FWHM giving a value of 1.3 ns.

From equation (1) one expects the elastic intensity to decrease continuously with temperature. As can be seen from Fig. 2 this is the case for bulk PG but not for the microemulsion. There, during the heating run the elastic intensity rises sharply at a temperature of 191 K to return to the original curve abruptly at 236 K. This is a clear indication of a ‘crystallisation gap’. Upon heating, as soon as the diffusion becomes fast enough, crystallisation takes place fixing the scatterers (predominantly hydrogen) into their lattice positions. This reduces the $\langle r^2 \rangle$ to the vibrational Debye-Waller factor-like contribution. When heating to the melting point, the scatterers become mobile again creating the second discontinuity. Considering the isomeric composition of the decalin used, it is clear that decalin is the crystallising component. The liquidus point for the given composition is 239 K [2] in non-deuterated *cis/trans* decalin. This coincides well with the high temperature end of the crystallisation gap found here. This also explains why crystallisation was not found in the earlier experiments of ref. 3. Commercial (non-deuterated) *cis/trans* decalin has a ratio of 77 : 23 which lies closer to the eutectic composition [2] of 62 : 38. For this reason, crystallisation is more efficiently suppressed when using commercial *cis/trans* decalin than for the specially synthesised deuterated we

used here.

Fortunately, the elastic scan method is fast enough that cooling from the liquid state avoids crystallisation. So by combining heating and cooling runs the whole temperature range can be covered. For all experiments involving longer registration times in the critical temperature range we looked out for indications of crystallisation. Although the crystallisation of decalin not necessarily affects the state of the PG inside the micelles we discarded all data where crystallisation took place.

By fitting equation (1) it is possible to calculate mean-square displacements from the elastic scans. This has been done with an additional Q^4 term in the exponential because the Gaussian expression was clearly unable to represent the data correctly at high temperatures. In addition only detectors with $Q \geq 0.5 \text{ \AA}^{-1}$ were considered to avoid an elastic contribution by the small-angle scattering from the droplet shape. To have the same definition of $\langle r^2 \rangle$ for the bulk its data was treated with the same restriction in Q . Also the necessary subtraction of ddd scattering from hdd made it impossible to correct for multiple scattering as it was possible for the bulk [1]. Nevertheless, the comparison with the more exact evaluation in Fig. 3 shows that there is no large error induced by the restrictions necessary here.

5 Multiple scattering correction

The resulting intermediate scattering function $S(Q, t)$ resulting from Fourier transform of the neutron scattering spectra was corrected for multiple scattering using the formula [4]

$$S(Q, t) = \hat{S}(Q, t) - \frac{s \cdot \overline{\hat{S}(t)^2}}{1 + s \cdot \overline{\hat{S}(t)}}. \quad (2)$$

Here, $\hat{S}(Q, t)$ is the uncorrected intermediate scattering function and s a parameter which in case of correct normalisation of the data represents the probability for second and higher scattering. The overline $\overline{\dots}$ denotes the solid-angle average. For the bulk sample the multiple scattering fraction was estimated in the usual way: Because the scattering is predominantly incoherent the low Q limit of $S(Q, t)$ should be

$$\lim_{Q \rightarrow 0} S(Q, t) = 1 \quad (3)$$

independently of t . Multiple scattering has the consequence that this limit falls below 1. It is now possible to determine the multiple scattering fraction by requiring that the limit (3) is fulfilled as good as possible by the corrected data.

The effect of the multiple scattering correction is demonstrated in Fig. 4. It can be seen that the correction becomes bigger for smaller Q . This is understandable because the (single) inelastic scattering decreases strongly with Q . Because the multiple inelastic scattering is roughly isotropic it becomes more and more important in proportion at low

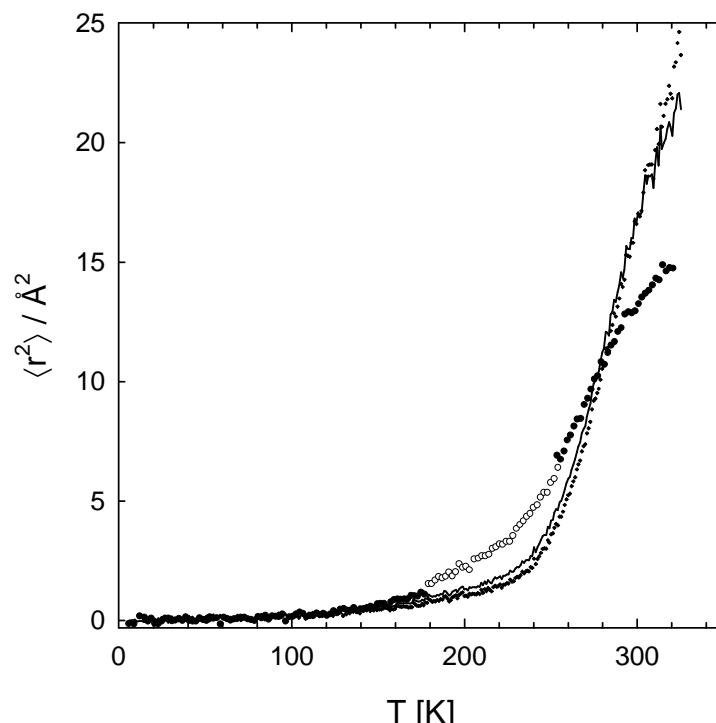


Figure 3: Mean-square displacements. The plotted $\langle r^2 \rangle$ results from fitting equation (1) with an additional Q^4 term to the spectra in the range $Q = 0.5 \dots 1.9 \text{ \AA}^{-1}$. Continuous line: bulk PG; filled symbols: confined PG heating scan; hollow symbols: confined PG cooling scan. Data of the heating run have been omitted in the range where data from the cooling run were available. The small diamond symbols show $\langle r^2 \rangle$ from an evaluation correcting for multiple scattering and using the whole Q range [1].

Q . What can also be seen is that the agreement between time-of-flight $S(Q, t)$ and that from backscattering improves by the multiple scattering correction. A direct comparison is not possible because the lowest obtainable time for backscattering is 150 ps and the highest for time-of-flight 20 ps. (This is an unavoidable consequence of the energy *range* of the backscattering spectrometer being narrower than the energy *resolution* of the time-of-flight spectrometer.) But from the connecting spline curves it is clear that there would have to be an artificial kink in the gap to reconcile the data sets without multiple scattering correction at low Q .

If for bulk PG the same fit as described in the main article is carried out on the $S(Q, t)$ *without multiple scattering* correction, the agreement with the data is significantly worse having about the double summed-square deviation. This results mostly from the small but in the fit noticeable mismatch between TOF and BS $S(Q, t)$. As in a study of polyisoprene [4] it turns out that the most sensitive parameter is ΔE_A which would be $235 \pm 5 k_B K$ without multiple scattering correction (as compared to $311 \pm 4 k_B K$). The other

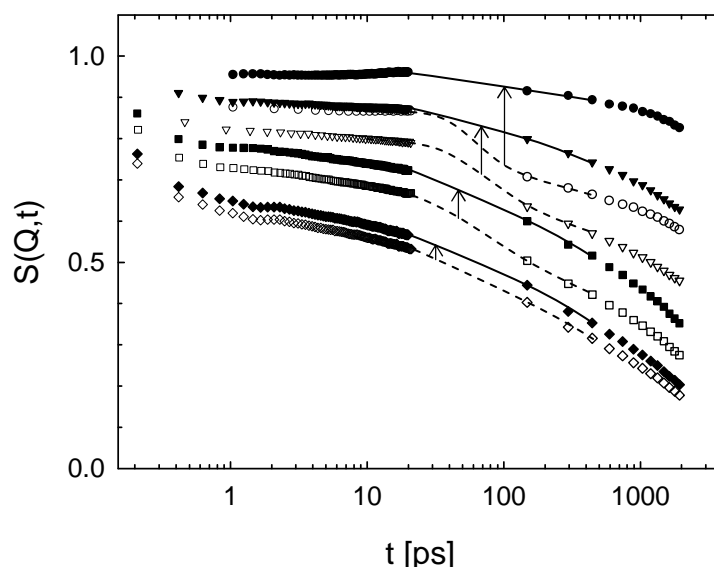


Figure 4: Comparison of ‘raw’ $S(Q, t)$ (hollow symbols) and multiple-scattering-corrected $S(Q, t)$ (filled symbols). Q values: circles 0.54 \AA^{-1} , triangles 0.87 \AA^{-1} , squares 1.42 \AA^{-1} , diamonds 1.88 \AA^{-1} . Points at $0.2 \dots 20$ ps stem from time-of-flight spectra (here: IN6) and those at $150 \dots 2000$ ps from backscattering spectra (here: IN16). The curves are guides to the eye in the gap between time-of-flight and backscattering data (dashed: non multiple scattering correction, continuous: multiple scattering corrected). The arrows show which curve is transformed into which and indicate the magnitude of the multiple scattering correction.

parameters are less significantly influenced. Their values would be $\tau_R^0 = (14 \pm 2) \times 10^{-15}$ s, $\beta = 0.627 \pm 0.009$, $E_A^0 = 2030 \pm 31 k_B K$ (instead of $\tau_R^0 = (5.8 \pm 0.8) \times 10^{-15}$ s, $\beta = 0.654 \pm 0.007$, $E_A^0 = 2273 \pm 28 k_B K$), and the τ_K values being less than $2 \dots 15\%$ smaller in the absence of multiple scattering correction. So we can conclude that if at all only the width of the energy barrier distribution for the methyl group reorientation could be affected by an uncertainty in the choice of the multiple scattering probability.

For the microemulsion-confined PG the multiple scattering correction was done (as for the bulk) on the intermediate scattering function $S(Q, t)$. But because this correction is non-linear it cannot be done on the difference of hdd and ddd data. Instead, it has to be done separately on both components with different multiple scattering probabilities.

The estimation of the multiple scattering fraction is much more difficult here since for coherent scattering the limit (3) does not hold. Fortunately for all experiments the sample shapes of the hdd and ddd samples were similar to that of the bulk sample. Because the parameter s in equation (2) should factorise into a sample-geometry dependent term and a scattering efficiency it is reasonable to assume that it is proportional to the total scattering within the series of samples. With this assumption it was possible to rescale

the multiple scattering probabilities of the bulk sample with the scattering efficiency (thickness \times scattering cross section) of the microemulsion samples to obtain the multiple scattering probabilities of the latter. It has to be noted that the uncertainty involved in this procedure does not affect the $S(Q, t)$ at high Q significantly because the total effect on the hdd-ddd difference is less than what is shown in Fig. 4 for the bulk.

6 Experimental difficulties

From the preceding data evaluation it is obvious that the system studied presents several complications. Although these problems are surmountable, for future studies improvements in the sample design may be in order.

(1) The small size of the microemulsion droplets causes them to show rather rapid diffusion which has to be taken into account in the evaluation of the dynamical data. As Fig. 4 and Table III of the main article show this induces some uncertainty in the evaluation of the data.

Also for comparison with previous studies in hard confinement a size of about 5 nm may be more suitable than the present extreme confinement.

Nevertheless a change of droplet size will not improve much the situation concerning the droplet diffusion because the diffusion coefficient scales only with $1/R$. A better solution may be to use an outer microphase with higher viscosity. But one has to observe that the T_g of this component still has to be lower than that of the inner microphase, a condition which excludes many high-viscosity liquids.

(2) The methyl sidegroup of PG causes an additional dynamics which at high temperatures is not well-separated from the α relaxation. For dielectric spectroscopy [3] this poses no problem because the methyl group does not have a dipole moment perpendicular to the rotation axis. But for inelastic neutron scattering it is clearly advantageous to have a confined material without extra degrees of freedom. The problem here is that such materials usually show a higher tendency of crystallisation.

(3) Despite the large neutron scattering cross section of the hydrogen nuclei in PG only 42% of the total scattering arises from PG. The reason is that the volume fraction of PG in the microemulsion is only 10%. This is a rather poor value compared to usual (hard) confining systems with filling factors of about 50% (e.g. nanoporous silica). The situation is aggravated for soft confinement by the fact that also the matrix exhibits a dynamics in the same time range as that of the confined material.

The solution found here is to perform the subtraction of a completely deuterated sample *after* Fourier transform. The advantages of this procedure are the following: (i) The exact amounts of hdd and ddd sample need not to be known. (ii) Multiple scattering corrections can be done on the $S(Q, t)$ of the hdd and the ddd sample separately. In this way the multiple scattering cross terms are treated correctly (which is not the case if the multiple scattering correction is done after subtraction). (iii) The treatment stays correct even if the instrumental resolution functions are different for hdd and ddd samples. These

advantages are partially compensated by the complication that the subtraction factors become Q dependent and can only be calculated if the scattering cross section is known in absolute units.

Although by this subtraction the matrix scattering can be safely corrected, the relative errors in the difference are much larger than in previous studies which employed hard confinement. In this respect the solution would be microemulsions with a higher concentration of droplets. But these are probably difficult to realise without having a tendency to convert into cylindric microemulsions at low temperatures.

References

- [1] R. Zorn, *Nucl. Instr. Methods A*, 2007, **572**, 874–881.
- [2] W. F. Seyer, S. Yip and G. Pyle, *J. Am. Chem. Soc.*, 1950, **72**, 3162–3164.
- [3] Li-Min Wang, Fang He, and R. Richert, *Phys. Rev. Lett.*, 2004, **73**, 095701-1–4.
- [4] R. Zorn, B. Frick, and L. J. Fetters, *J. Chem. Phys.*, 2002, **116**, 845–853.